ACADEMIC PRESS

Available online at www.sciencedirect.com
SCIENCE DIRECT®

Journal of Catalysis 215 (2003) 20–29

JOURNAL OF CATALYSIS

www.elsevier.com/locate/jcat

A periodic density functional theory study of thiophenic derivative cracking catalyzed by mordenite

Xavier Rozanska,[a,*] Rutger A. van Santen,[a] François Hutschka,[a,b] and Juergen Hafner [a,c]

[a] *Schuit Institute of Catalysis, Laboratory of Inorganic Chemistry and Catalysis, Eindhoven University of Technology, PO Box 513, NL5600 MB Eindhoven, The Netherlands*

[b] *Totalfinaelf, Raffinerie des Flandres, Département Technique, Secteur Technique no 4, BP 79, F59279 Loon Plage, France*

[c] *Institut für Materialphysik, Universität Wien, Sensengasse 8, A1090 Vienna, Austria*

Received 4 July 2002; revised 31 October 2002; accepted 31 October 2002

Abstract

A periodic density functional theory study of thiophenic derivative cracking catalyzed by proton- or lithium-exchanged mordenite has been performed. The same qualitative trends in activation energies as those described employing the cluster approach method have been obtained. However, the zeolite framework appears not to stabilize the transition state complexes. This is explained by the zwitterionic nature of the thiophenic derivatives cracking transition state complexes. The zeolite framework has more subtle effect on reactivity, as shown by the alteration of the ionic nature of the transition state complex in the case of better fit with the zeolite cavity. Notwithstanding, thiophenic derivative cracking catalyzed by zeolites remains difficult. General comments concerning the use of zeolite catalysts in hydrodesulfurization are made. Predictions on zeolite-based catalysts more suitable to achieve hydrodesulfurization are described.

Keywords: Zeolite; Mordenite; DFT calculations; Quantum chemistry; Desulfurization; Cracking; DBT; Dibenzothiophene; Thiophene

1. Introduction

Hydrodesulfurization (HDS) of thiophenic derivatives has been the subject of many studies these past years [1–20]. The driving force for the investigation of these systems arises from the industrial need to improve HDS processes of petroleum feedstock in order to provide low-sulfur-content transportation fuel [1]. New environmental regulations that are stricter regarding transportation fuel composition are the main reason for this demand [1,2].

Sulfur is present as thiols and thiophenic derivatives in feedstock [3,4]. The fraction of sulfur existing as thiols, thiophene, and alkylated thiophenes is rather easily hydrodesulfurized in the classical HDS. Sulfur in polyaromatics (i.e., benzothiophene derivatives) shows a stronger resistance to HDS. In the case of multialkylated polybenzothiophene molecules, the HDS resistance even turns into high refraction [3–8].

Usually, HDS catalysts consist of a sulfidic Ni–Mo or Ni–W phase dispersed over a γ-alumina or zeolite support [1,5,8]. The activity of this class of catalysts in HDS has been known for years. However, little understanding of the reason for its activity at the molecular level was available [5]. The industrial pressure to develop more efficient catalysts to achieve deep hydrodesulfurization led to a renewal of scientific interest in this class of catalysts. During the past years, this resulted in a large number of theoretical studies, which give better insight into the molecular description of HDS [9–13].

Interestingly, it has been found that zeolites alone can catalyze HDS [14–20]. Zeolites are microporous (alumino)silicate crystals [21–23]. Because they are silicates, they show good thermal and mechanical properties, which make them appropriate catalysts or catalyst supports [24]. Furthermore, their well-characterized microporous network is the reason they are commonly employed as molecular sieves [21]. This property is also particularly useful in catalysis, whether zeolites are catalysts or catalyst-supports, as it induces shape selectivity reactions [25–28]. Zeolites can act themselves as catalysts: a fraction of framework silicon atoms are naturally found to be substituted for +III (viz., Al)- or +IV (viz., P)-valent atoms. Cations or anions are introduced to neutralize the framework charge. The catalytic activity of zeolites will

* Corresponding author.
E-mail address: tgakxr@chem.tue.nl (X. Rozanska).

0021-9517/03/$ – see front matter
doi:10.1016/S0021-9517(02)00148-3

depend upon the nature of these cations or anions. Lewis and/or Brønsted basic and/or acidic sites are then generated.

Proton-exchanged aluminosilicate zeolites are solid acid catalysts commonly used in alkane or olefin hydroforming (viz., hydroisomerization and hydrocracking) and in aromatic conversion (viz., isomerization, alkylation, and transalkylation) [29]. Their activity in HDS has been experimentally tested [14–20]. Furthermore, bifunctional catalysts, combining a classical HDS catalyst dispersed over a proton-exchanged zeolite catalyst, have been considered [3,4,6, 14–17]. The hydrodesulfurization rate of the HDS refractory 4,6-dimethyldibenzothiophene was significantly increased when such a bifunctional catalyst was employed [3,4,6]. Michaud et al. [6] and Landau [3] explained this result by the isomerization of 4,6-dimethyldibenzothiophene, which led to molecules in which the thiophenic sulfur atom was not longer hidden behind the alkyl groups. Thus, HDS catalysts could more easily convert isomerized dimethyldibenzothiophene.

However, the actual relationship between the two constituents of the bifunctional catalyst turns out to be more complicated than the above-mentioned description. Welters et al. [16,17] reported that the rate of dibenzothiophene HDS increases linearly with the acid strength of the proton-exchanged zeolite. The basis for the synergy between the protonic zeolite and the HDS catalyst remains unclear.

In an attempt to rationalize hydrodesulfurization of thiophenic derivatives by zeolite catalysts, Saintigny et al. [30] and Rozanska et al. [31,32] performed quantum chemical studies of the different reaction paths. As they used a cluster model of the zeolite catalyst in their theoretical calculations, they could only provide qualitative trends. They demonstrated the importance of H_2 and thiophene hydrogenation in HDS. They observed that the zeolite catalytic center in thiophenic derivative HDS is a Lewis basic site, and that Brønsted acidity plays a limited role in this reaction. These quantum chemical results are supported by experimental studies. It has been identified by Vrinat et al. [14] and Ono [18] that proton-exchanged zeolites are not the most efficient catalysts in thiophene and dibenzothiophene cracking. Zeolites with stronger Lewis basic sites showed a faster reaction rate. The effect of H_2 in thiophene HDS has been illustrated in the investigations of Yu et al. [20].

Our objective is to extend the analysis of desulfurization of thiophene derivatives catalyzed by a zeolite. It has been shown that thiophenic ring cracking is the rate-limiting reaction step in thiophene and dibenzothiophene hydrodesulfurization (see Scheme 1) [30–32]. We will here limit our investigations to this reaction. We used in the previous studies [30–32] a small molecular fragment as a model of the zeolite catalyst that aims to model the catalytic active site. This method, known as the cluster approach method, has been shown to give good qualitative data [33–37]. In the present study, periodic electronic density functional theory calculations of thiophene, dihydrothiophene, and dibenzothiophene cracking catalyzed by proton- and lithium-exchanged mordenite will be presented. This will allow us to describe the interaction between transition state complexes and zeolite framework, providing further insights into zeolite-catalyzed reactions and thiophenic derivative hydrodesulfurization.

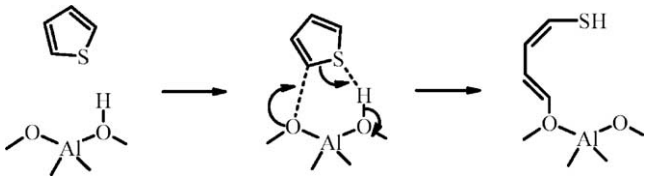

Scheme 1. Reaction mechanisms in the cracking of thiophenic rings catalyzed by acidic zeolites.

An important feature in zeolite catalysis is the stabilization of carbocation-like transition state complexes by the zeolite framework. With the periodic density functional theory method, we are able to describe this effect [35,37,38]. Moreover, as the repulsive contribution is treated at the quantum chemical level, it is possible to describe steric constraints in zeolites accurately. However, density functional theory methods are known to describe London dispersion forces inaccurately [22,23,34–38]. It was shown by Klein et al. [39] that the van der Waals contribution remains almost constant in aromatic adsorption within zeolite. London forces can be assumed to be approximately constant on intermediates and transition states, whereas zeolite electrostatic and repulsion contributions can dramatically alter the picture [23,34,35,37,40,41]. We selected mordenite as catalyst [34–36]. This zeolite has large microcavities that can accommodate the large dibenzothiophene molecule. Moreover, the unit cell that characterizes this crystal is small (i.e., 144 atoms), which facilitates the calculations.

2. Method

The periodic density functional theory calculations are performed employing the Vienna ab initio simulation package (VASP) [42–45]. The total energy is calculated solving the Kohn–Sham equations using the local exchange–correlation functional proposed by Perdew and Zunger [46]. The results are corrected for nonlocality in the generalized gradient approximation with the Perdew–Wang functional (PW91) [47]. VASP uses plane waves and ultrasoft pseudopotentials [48]. A 300-eV energy cutoff and a Brillouin-zone sampling restricted to the Γ-point were selected in our calculations.

The mordenite zeolite structure used in the calculations is similar to the one that has been used before [34–36]. The dimensions of the unit cell are $a = 13.648$ Å, $b = 13.672$ Å, $c = 15.105$ Å, $\alpha = 96.792°$, $\beta = 90.003°$, and $\gamma = 90.022°$. The Si/Al in this mordenite model is 23. It is the same mordenite model as in previous studies [34–36]: this allows straight comparison between the different studies, as acidic strength of zeolite varies with Si/Al ratio [22,23,29]. The Brønsted sites have been selected, as before, at the junction

of 12- and 8-member rings, as these sites are the most stable [49]. The position of the proton participating in the reaction has been selected to allow the formation of alkoxy species at the most accessible oxygen atom (i.e., at the junction of two 8-member rings). The position of the proton around the aluminum is of limited importance due the relatively mobility of protons in zeolites [40,50]. The second Brønsted site does not get involved in the reaction.

Relaxation of the adsorbed compounds and intermediates was performed employing a quasi-Newton algorithm based on analytical forces minimization. Convergence was assumed to be reached when forces were below 0.05 eV/Å.

The transition state search method in VASP is the nudged elastic band method [51]. Several images of the system are defined along the investigated reaction pathway. These images are optimized, but only allowed to move in the direction perpendicular to the vector defined by the hypertangent between their two neighboring images. We employed up to eight images to analyze potential energy surface in the surrounding of the transition state. When forces on the system images were below 0.08–0.10 eV/Å, the image with the maximum energy in the reaction pathway was separately optimized using forces minimization.

3. Results

3.1. Thiophene cracking

We selected the geometry of thiophene in contact with the zeolite catalytic site based on experimental and theoretical results. It has been observed that thiophene or any other thiophenic derivative adopts an η^1(S) adsorption mode with respect to the zeolitic proton [19,52]. The geometry and main geometrical parameters of the optimized system can be seen in Fig. 1 (see Ads_thio1).

The transition state reaction pathway in the nudge elastic band calculations has been defined following earlier experiences [30,31]. Furthermore, alternative reaction pathways were checked. For instance, one could imagine that the zeolite framework could strongly stabilize protonated thiophene. Then, thiophenic ring cracking will proceed after a protonation step. These assumptions appear to be wrong, and the reaction mechanism that is more likely is similar to that in the cluster approach calculations [30,31]. Lewis basic oxygen atom induces thiophenic ring cracking, whereas the acidic proton position does not change much in the transition state (see TS_thio1 in Fig. 1).

The activation energy for thiophene cracking is 318 kJ/mol. One notes that this value is higher than that was previously reported [30,31]. The thiophene cracking activation energy has been calculated to be around 226 kJ/mol using the cluster approach method [31]. This is rather unexpected as so far it is commonly thought that the zeolite framework stabilizes transition state structures. Later in the discussion, we will provide an explanation.

Thiophene cracking leads to the formation of an alkoxy species (see Alk_thio1 in Fig. 1). This species is not very stable and undergoes thiol-formation with the assistance of H_2 [30]. The energy of this system is +128 kJ/mol with respect to physisorbed thiophene. This energy difference is similar to that found in the cluster approach calculation [31]. This is in agreement with previous quantum chemical studies. It has been noted that the energy of a neutral system is almost unaffected when more realistic zeolite models are used in the calculations [34–37].

We observed in previous cluster approach calculations [31] and in agreement with experimental data [14–20] that

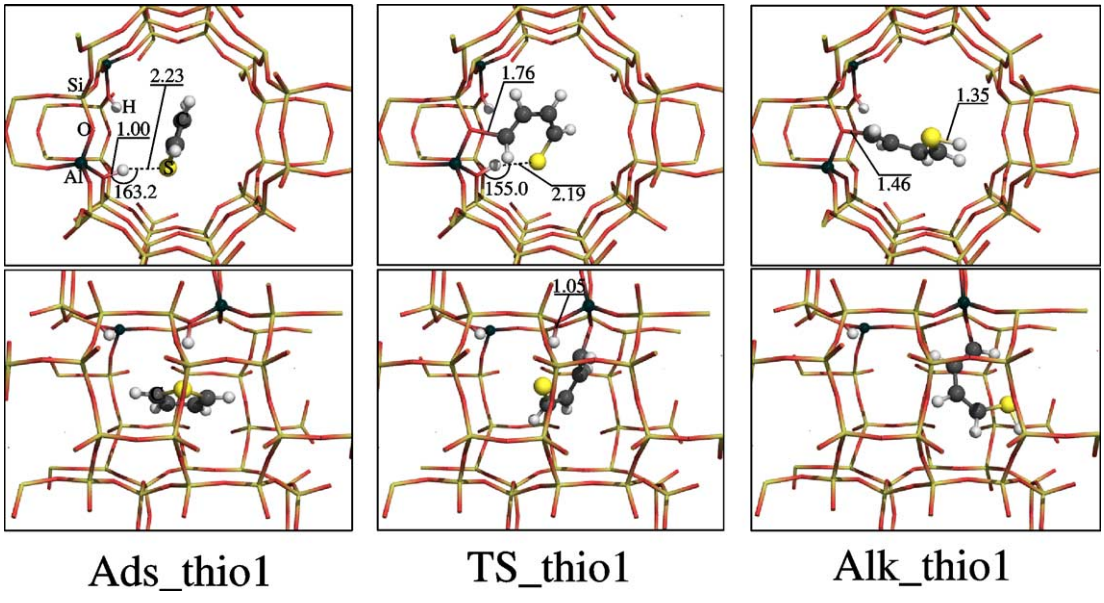

Fig. 1. Intermediates and transition state geometries and main geometrical parameters in thiophene cracking catalyzed by proton-exchanged mordenite.

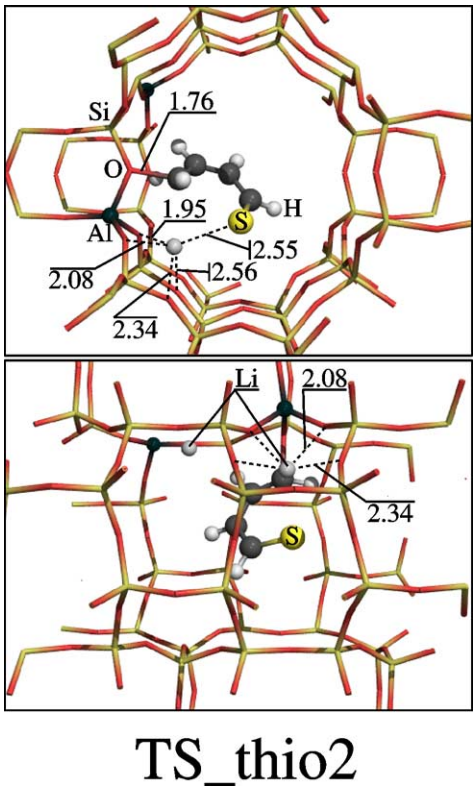

Fig. 2. Transition state geometry and main geometrical parameters in thiophene cracking catalyzed by lithium-exchanged mordenite.

cation-exchanged zeolites other than proton-exchanged ones can more easily induce thiophene cracking. We considered this case for a lithium-exchanged zeolite catalyzed reaction. The geometry of the optimized transition state is shown in Fig. 2. One notes that the Li^+ cations are in interaction with as many zeolitic oxygen atoms in mordenite as possible. The Li^+ cation that is active in the reaction has an η^5 adsorption mode. The inactive Li^+ cation has an η^8 adsorption mode and is located in the center of an eight-ring side pocket of mordenite (see Fig. 2). It was not our objective in this study to analyze the stability of the different locations of Li in mordenite. Barbosa et al. [53] and others [54,55] achieved quantum chemical studies dedicated to this subject.

The activation energy in thiophene cracking by Li-exchanged mordenite is 280 kJ/mol (*versus* 205 kJ/mol in the cluster approach calculations) [31]. This is 38 kJ/mol lower than the activation energy by the proton-exchanged mordenite in the periodic calculations. The difference in activation energies between these reactions was 21 kJ/mol in the cluster approach calculations [31].

3.2. Dihydrothiophene cracking

We have shown that pre-partial hydrogenation of the thiophene ring in thiophene [31] or in dibenzothiophene [32] was helpful in lowering the thiophene ring cracking activation energy. We noted that full hydrogenation of the thiophene ring in thiophene does not lead to a further decrease of the activation energy [31]. This was explained because only a C–S bond was broken in the thiophenic ring cracking. Partial hydrogenation led to weakening of a C–S bond, which became more easily breakable.

The geometry and main geometrical parameters of dihydrothiophene are shown in Fig. 3. An η^1(S) adsorption mode for dihydrothiophene physisorbed to the acidic proton was selected.

The transition state search in dihydrothiophene was carried on as in the case of thiophene cracking. One notes that the optimized geometries of the transition state complexes in thiophene and in dihydrothiophene show similarities and differences (see Figs. 1 and 3). Similarities are the zwitterionic nature of the transition state complexes: in thiophene as well as in dihydrothiophene cracking. The proton is still bonded to the zeolite framework, the C–S bond is clearly broken, and the C-zeolite O alkoxy bond is not fully formed. Then, the thiophenic derivatives charge is negative on the sulfur atom, and positive on the C1 carbon atom (see Scheme 1). Meanwhile, the zeolitic catalytic site shows geometry close to the undisturbed case. The difference is the larger ability of dihydrothiophene to adopt other configurations, as two carbon atoms in the thiophenic ring are now sp^3 hybridized. Molecular rotations around these carbon atoms induce dihydrothiophene to more easily accommodate its geometry to the zeolite framework. As can be seen in Fig. 3, the sulfur atom almost becomes involved in a hydrogen bond with the spectator Brønsted acidic site.

The activation energy in dihydrothiophene cracking is 272 kJ/mol. Once more, the same qualitative trend was obtained in cluster approach calculations [31]. Lowering of the activation energy in dihydrothiophene cracking was around $\Delta E_{act} = -12$ kJ/mol. In the periodic calculations, it is more significant with $\Delta E_{act} = -36$ kJ/mol. However, as in thiophene cracking, the dihydrothiophene cracking activation energy appears to be higher in the periodic calculations than in the cluster approach calculations (E_{act}s are 272 and 214 kJ/mol, respectively) [31].

The energy of the thiol–alkoxy species, the product of the dihydrothiophene cracking, is +128 kJ/mol with respect to physisorbed dihydrothiophene. This is very close to the reaction energy obtained in cluster approach calculations [31]. Here, we obtained a reaction energy of 108 kJ/mol.

3.3. Dibenzothiophene cracking

Mordenite 12-membered parallel channels are well suited to accommodate the large dibenzothiophene molecule (see Fig. 4). Dibenzothiophene can fit without dramatic steric constraints in the microcavity. However, as we will see, this is not the case once the thiophenic derivative has cracked, and chemisorbed to the zeolite wall.

Physisorbed dibenzothiophene main geometrical parameters (see Fig. 4) are very similar to those observed in thiophene (see Fig. 1) or in dihydrothiophene (see Fig. 3).

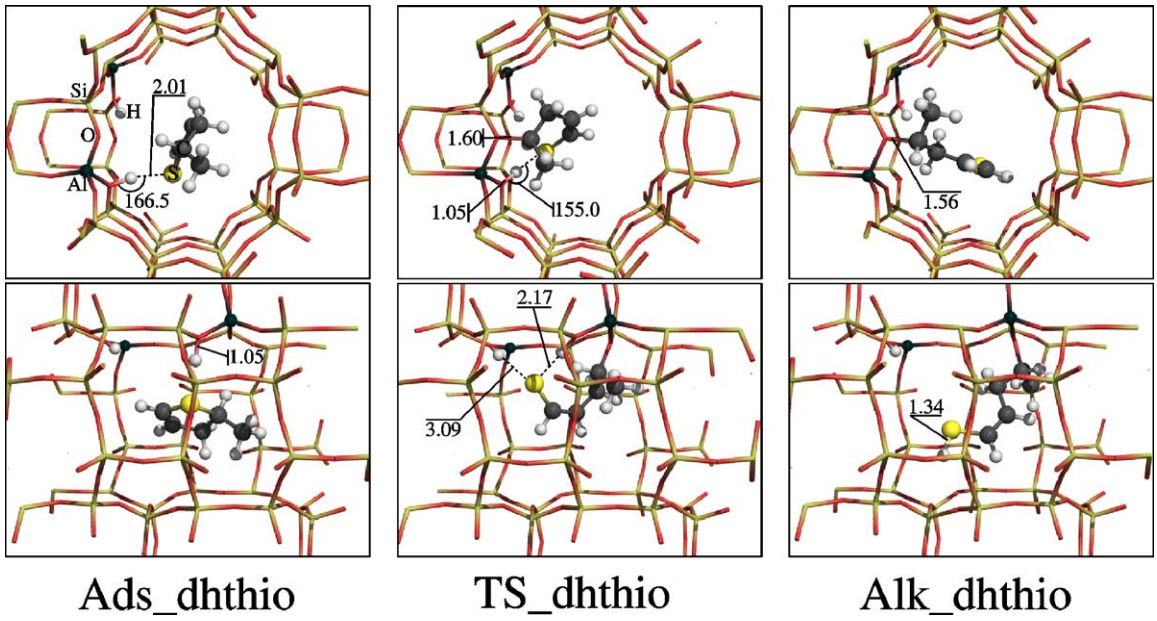

Fig. 3. Intermediates and transition state geometries and main geometrical parameters in dihydrothiophene cracking catalyzed by proton-exchanged mordenite.

The validity of the comparison between the different thiophenic derivatives stops there.

In the optimized transition state complex (see TS_dbt in Fig. 4), the alkoxy bond formation is very far from completion: C–O is 2.31 Å, whereas it is 1.76 and 1.60 Å in thiophene and dihydrothiophene transition state complexes, respectively. Also, the proton is already connected to the thiophenic sulfur atom (C–S = 1.38 Å), contrary to what was previously observed (C–S = 2.19 and 2.17 Å in thiophene and dihydrothiophene transition state complexes, respectively). The dibenzothiophene transition state complex does not constitute a zwitterionic complex as was observed in thiophene and in dihydrothiophene, and as was also observed in the dibenzothiophene transition state complex found in the cluster approach calculations [32]. This alternative transition state complex mechanism was also tested in the case of thiophene and dihydrothiophene but it is only found with dibenzothiophene in mordenite to be more likely.

The dibenzothiophene cracking activation energy is 314 kJ/mol. This is close to what was obtained in thiophene cracking (viz., $E_{act} = 318$ kJ/mol), but slightly higher than

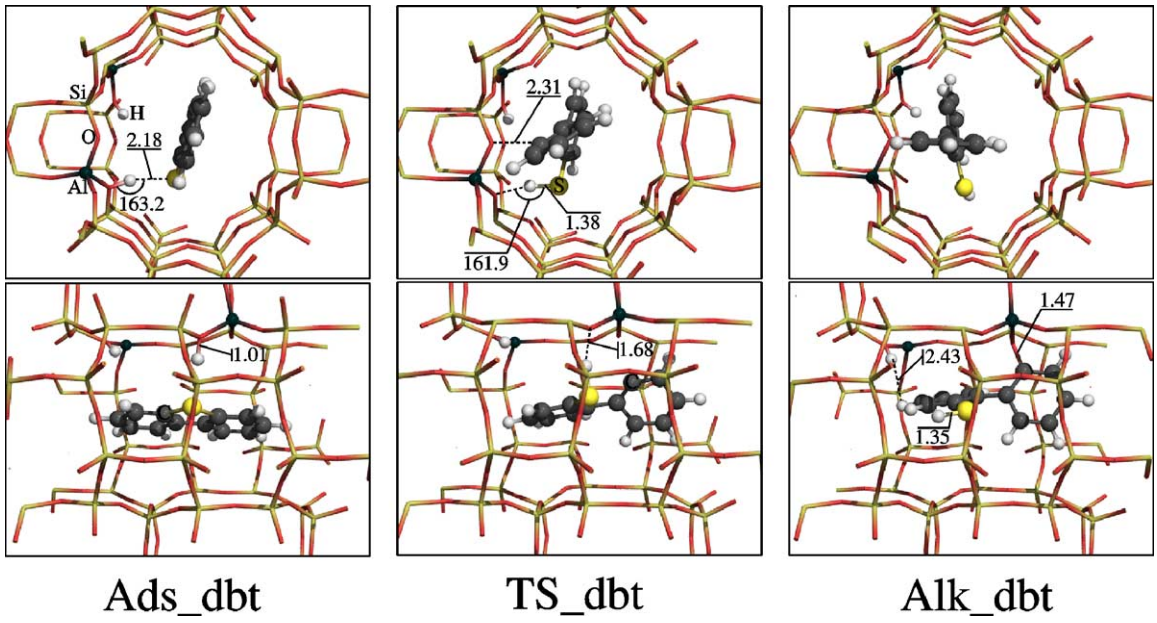

Fig. 4. Intermediates and transition state geometries and main geometrical parameters in dibenzothiophene cracking catalyzed by proton-exchanged mordenite.

that was obtained in the cluster approach calculations (viz., $E_{act} = 288$ kJ/mol) [32].

The geometry and main geometrical parameters of the chemisorbed thiol molecule formed after dibenzothiophene cracking can be seen in Fig. 4 (see Alk_dbt). The alkoxy bond is itself similar to that is measured in thiophene or dihydrothiophene alkoxy species. However, the dibenzothiophene alkoxy species suffers from strong steric constraints: its energy is +180 kJ/mol with respect to physisorbed dibenzothiophene, whereas it was only +90 kJ/mol according to cluster approach calculations [32]. As we already mentioned, neutral systems are expected to remain at similar relative energy levels when a more realistic zeolite model is employed [33–37]. A closer look at the alkoxy species in periodic (see Fig. 4) and in cluster approach calculations [32] reveals immediately the deformation of the geometries due to the zeolite steric constraints.

4. Discussion

Two important issues will be discussed in this section. First, we will analyze the data that have been obtained on hydrocarbon catalysis by zeolites; especially, interactions between the transition state complexes and the zeolite framework will be estimated. Second, on a less important topic, we will consider the thiophenic ring cracking catalyzed by zeolite. Confrontation of our data with others, understanding of the nature of the transition complexes, and influence of the

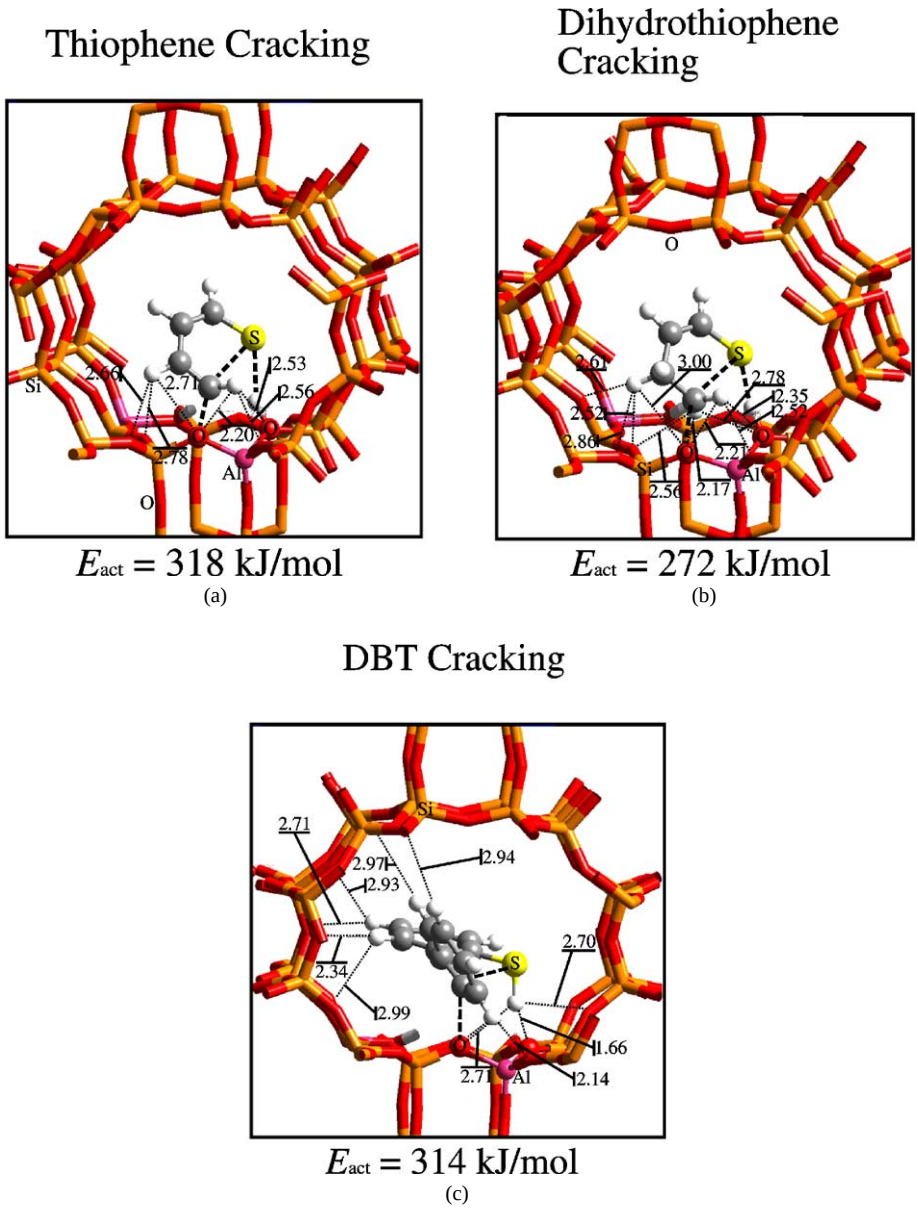

Fig. 5. Details of the geometries of the cracking transition states of thiophene (a), dihydrothiophene (b), and dibenzothiophene (c). The distances between thiophenic derivatives H atoms and zeolite O atoms are reported.

catalyst will allow us to elaborate general comments on this reaction.

4.1. Interaction between cracking transition states and zeolite framework

We have shown in previous theoretical studies the effect of the zeolite framework on the stabilization of transition state complexes [31–38,56,57]. Briefly, the zeolite framework stabilizes carbocationic transition state complexes. The main contributions that favor this stabilization are short-range electrostatic contributions, among which especially zeolite oxygen atoms induced dipoles–transition state complex charge interaction. As this energy stabilization is dominated by short-range interactions, the TS stabilization is dependent on the zeolite structure: in agreement with previous concepts developed in zeolite catalysis [22,23], we noted that stabilization of given transition state complexes were dependent on the size of the zeolite cavities [57].

To estimate the effect of the zeolite micropore size and shape on the stabilization of transition state structure is to consider the situation in another way. Different thiophenic derivatives were considered in the present study, whereas the zeolite catalyst remained the same. The comparison of the data that are obtained using the periodic DFT method with those of the cluster approach method [30–32] is especially revealing when transition states of different size are compared, as the zeolite framework is not described in the cluster approach calculations. Thus, one can estimate the effect of the zeolite framework on the reaction.

Let us more closely monitor the structure of the transition state complexes and zeolite framework. The geometries of cracking transition state are shown in Fig. 5. The thiophene transition state structure is not in close interaction with the zeolite wall. The dihydrothiophene transition state experiences more contact with the zeolite wall. The dibenzothiophene transition state interacts with all sides of the zeolite micropore. The geometries of the transition states of cracking of thiophene and dihydrothiophene are very much like those of cluster approach method calculations. In the case of dibenzothiophene, a major difference occurs: in the periodic system, the sulfur atom has become protonated in the transition state, contrary to what is observed in the cluster approach calculations.

A surprising result concerning the thiophenic derivative cracking calculations is that transition state structures are no longer stabilized by their interactions with the zeolite framework (see Table 1). This follows when cluster approach results are compared to periodic results. Let us consider dibenzothiophene as a specific case: as can be seen from the energy difference between physisorbed system and alkoxy species, large steric constraints are involved in this system. We will achieve the analysis of dibenzothiophene cracking a bit later.

The source of the destabilization of the thiophenic-ring-cracking transition state in thiophene and dihydrothiophene is clarified when further analysis of the systems is achieved. In Table 2, we used the transition state structures that are similar in both cluster and periodic approaches [31,33,35,36,38]. The cracking DBT transition state structure is not reported in this table, as it is not similar in both approaches. We will come back to this point later. The limited model of the Mulliken charges is employed here to describe the carbocationic nature of different hydrocarbon transition states. The charge is calculated by adding the separate charges carried by atoms in the transition state structure in the cluster approach calculations. The comparison between the Mulliken charges and the differences in the activation energies between cluster and periodic approaches shows an interesting trend [30,33] (see Table 2). We previously identified that the positive charge in the carbocation-like transition state induces polarization of the zeolite oxygen atoms [35,38]. Hence, more charge separation in the transition state should lead to an increase of the zeolite-framework-induced-dipoles–transition state charge electrostatic contribution. However, when the charge separation in the transition state is not sufficient, this stabilization should turn into a destabilization. As we previously mentioned, thiophenic derivative cracking transition state complexes are different from other carbocationic transition state complexes because they are zwitterion-like transition state complexes. The activation energies in Table 2 have been obtained using different density

Table 1
Calculated thermodynamic data in cracking of thiophenic derivatives catalyzed by acidic zeolite[a]

Reactant	E_{act}		ΔE	
	Periodic[b]	Cluster[c]	Periodic[b] (chemisorbed–physisorbed)	Cluster[c] (chemisorbed–physisorbed)
Thiophene	318	226	128	108
Dihydrothiophene	272	214	83	73
DBT	314	288	180	90

[a] All data in kJ/mol. See Scheme 1 for description of intermediates and transition state.
[b] This study.
[c] See Refs. [31,32].

Table 2
Comparative analysis of energy stabilization of some transition states by zeolite frameworks and of Mulliken charge in the corresponding transition state structure

Reaction	Mulliken charge	ΔE_{act}[a] (periodic-cluster)	Source
Thiophene cracking	0.25	92	[31] and this study
Dihydrothiophene cracking	0.28	58	[31] and this study
Propylene chemisorption	0.60	−34	[23,38]
Toluene isomerization	0.88	−100	[33,35]

[a] In kJ/mol; activation energies in this difference have been obtained using different methods. Therefore, only the qualitative trend should be considered.

functional theory methods. Employing the same method should result in different quantitative results; also the qualitative trend should be respected.

Comparison of thiophene and dihydrothiophene cracking reveals that the size of the transition state is important. There are two additional hydrogen atoms in dihydrothiophene compared to thiophene. Dihydrothiophene cracking transition state structure destabilization is 58 kJ/mol, whereas it is 92 kJ/mol for thiophene. This large difference is not explained by the difference in the Mulliken charge. Additional hydrogen bonds between activated dihydrothiophene and the zeolite framework can explain this stronger stabilization in part. For the other part, the higher ability of dihydrothiophene to adapt its geometry to the zeolite framework also probably favors a stronger energy stabilization of the transition state complex. However, it is difficult to estimate the relative importance of each of these contributions in the stabilization.

In dibenzothiophene, we mentioned that steric constraints alter the picture. However, we developed an approach that was revealed to be useful and reasonably accurate for estimating and correcting for this change [37,56,57]. For this purpose, the Polaniy–Evans–Brønsted relation is employed [23,58,59].

Application of this corrective method leads to an estimated value of dibenzothiophene cracking in the absence of steric constraints of the order of $E_{act} \sim 270$ kJ/mol. The dibenzothiophene cracking transition state structure is actually slightly stabilized in its contact with the zeolite framework. We mentioned that contrary to what was obtained in cluster approach calculations, dibenzothiophene was protonated in the periodic transition state. Therefore, the charge separation is more complete in this transition state than in the cluster approach transition state. Furthermore, the transition state structure fit to the micropore is better than for thiophene or dihydrothiophene.

It is extremely important to mention that the relation between charge separation in the transition state and transition state energy stabilization must be handled with caution. Qualitatively, it is correct. However, we described that other factors play also an important role in the transition state stabilization. These are the size of the transition state structure (number of H atoms in the hydrocarbon molecule) and the dimensions of the zeolite micropore. Moreover, changes in transition state complexes such as in dibenzothiophene cracking cannot be a priori predicted. Further systematic studies are required in order to develop an estimate of the importance of these different contributions.

4.2. Thiophenic derivatives cracking catalyzed by zeolites

In this section, we will put in perspective the results that have been obtained in thiophenic cracking quantum chemical calculations using a realistic model of zeolite catalysts. We report activation energies relevant to hydrodesulfurization of thiophenic derivatives in Table 3. Activation energies of thiophenic derivatives cracking by zeolite catalysts are from the present study. Ángyán et al. [60] performed periodic quantum chemical calculations for hydrocarbons (viz., ethane, propane, and butanes) catalyzed by proton-exchanged chabazite. We summarize their results in Table 3. We mentioned their data as they have been obtained using the same quantum chemical method than in our studies. Moreover, these data are in good quantitative agreement with experimental hydrocracking activation energies [60]. The isomerization of alkylated benzothiophene derivative activation energies comes from one of our previous periodic quantum chemical studies [36]. All these data have been obtained using the VASP program.

Table 3
Trends in activation energies of reactions related to hydrodesulfurization based on reported data

Reaction–catalyst	Activation energy (kJ/mol)	Source
Thiophenic derivatives cracking by zeolite	270–320	(This study)
Hydrocarbons cracking by zeolite	150–220	[60]
Alkylated thiophenic derivatives isomerization by zeolite	135–165	[36]
Thiophene HDS by metal sulfide	240–300	[61–65]

Concerning the activation energies of hydrodesulfurization of thiophene by classical HDS catalysts (viz., Mo, Co, CoMo, and Rh sulfides dispersed over a carbon support), we refer to the experimental data of Hensen et al. [61,62]. As the data they presented are apparent activation energies, we had to correct these from adsorption energies of thiophene so as to get activation energies. For this purpose, we used data of theoretical studies [63,64] (see also Ref. [65]).

One can see in Table 3 that zeolite catalyst can crack thiophene derivatives, but the activation energies are higher than those required when metal sulfide is employed ($\Delta E_{act} \sim 30$ kJ/mol).

Isomerization of alkylated benzothiophene derivatives activation energies is much lower than hydrodesulfurization activation energies ($\Delta E_{act} \sim 65$–85 kJ/mol). In agreement with experimental data [3,4,6], it is predicted that isomerization prior hydrodesulfurization in HDS of multialkylated polyaromatic thiophenic derivatives catalyzed by a bifunctional catalyst is likely to occur.

However, when the data of Ángyán et al. [60] are considered, a difficulty in this clear picture becomes apparent. Activation energies of alkane cracking catalyzed by proton-exchanged zeolite overlap with the alkylated aromatic thiophenic derivatives activation energies. Actually, the differences in activation energies indicate that isomerization will certainly take place. However, the concern is about the product of the HDS reaction: these are alkanes. The presence of acidic zeolite catalytic sites will crack HDS products. This may lead to a substantial lowering of the quality of transportation fuel.

Zeolite catalysts as such are not very good catalysts in HDS of thiophenic derivatives. We saw that the zwitterionic

nature of the cracking transition state complex disfavored the occurrence of this reaction in zeolite microcavity. However, the understanding of the transition state structure is very helpful in case one wants to tune zeolite catalyst activity specifically to this reaction. The difference in activation energies between a (nonadapted) zeolite and metal sulfide catalysts is relatively small, and can be further decreased.

5. Conclusions

We have performed a periodic density functional theory study of thiophene, dihydrothiophene, and dibenzothiophene catalyzed by mordenite.

The same qualitative trends in activation energies such as those observed in cluster approach calculations [30,32] are obtained. This confirms again [33,37] the validity of the cluster approach method in predicting qualitative results in zeolite-catalyzed reactions. These trends are also confirmed by experimental data [14,20].

However, the zeolite framework does not have a stabilizing effect on the transition state complexes of the thiophenic derivatives cracking. This is explained by the zwitterionic nature of the transition state complexes. Zeolite framework has a consequent stabilizing effect of carbocationic transition states as indicated in aromatic conversion [33,37,56], or olefin chemisorption [38,57] for instance.

The thiophenic derivative cracking activation energies are observed to be in the range 270–320 kJ/mol. These are higher than those that are experimentally measured when metal sulfide(s) catalysts are employed [61–65]. The difference in activation energies is evaluated to be around 30 kJ/mol. One predicts, considering that the zeolite framework is not well suited to favor zwitterionic-transition state complexes, that more favorable conditions can be met to allow competitive zeolite-based hydrodesulfurization. These conditions could be the chemical modifications of the zeolite framework or the use of adapted ancillary molecule(s).

Proton-exchanged zeolite catalysts appear not to be a so-good catalyst in hydrodesulfurization. The problem issues from side reactions (viz., olefin and alkane cracking, oligomerization, cyclization, etc.) that are also catalyzed by proton-exchanged zeolite [66,67]. All these side reactions are more easily undertaken by proton-exchanged zeolite than thiophenic derivatives cracking. They are damaging to the quality of the end-product (i.e., transportation fuels). One can note that these side reactions involved carbocationic and not zwitterionic transition states.

An interesting result is obtained when the fit of the transition state complex with the zeolite cavity varies. We considered the case of thiophene, dihydrothiophene, and dibenzothiophene cracking by mordenite. The size of the transition state changes drastically from one molecule to another. With dibenzothiophene cracking, the transition state complex is altered because of its contact with the zeolite cavity and is changed into a carbocationic transition state complex. While the steric constraints partly destabilize the reaction, the zeolite electrostatic contribution stabilizes the transition state structure.

Acknowledgments

Computational resources were partly granted by the Dutch National Computer Facilities (NCF). This work was performed within the European Research Group “Ab Initio Molecular Dynamics Applied to Catalysis,” supported by CNRS, IFP, and Totalfinaelf. X. R. thanks Totalfinaelf for the financial support.

References

[1] K.G. Knudsen, B.H. Cooper, H. Topsøe, Appl. Catal. A 189 (1999) 205.
[2] T. Takatsuka, S.-I. Inoue, Y. Wada, Catal. Today 39 (1997) 69.
[3] M.V. Landau, Catal. Today 36 (1997) 393.
[4] M.V. Landau, D. Berger, M. Herskowitz, J. Catal. 158 (1996) 236.
[5] T. Weber, R. Prins, R.A. Van Santen, Transition Metal Sulphides, Chemistry and Catalysis, in: NATO ASI Series 3, Vol. 60, Kluwer Academic, Dordrecht, 1998.
[6] P. Michaud, J.L. Lemberton, G. Pérot, Appl. Catal. A 169 (1998) 343.
[7] V. Meille, E. Schulz, M. Lemaire, M. Vrinat, J. Catal. 170 (1997) 29.
[8] P.T. Vasudevan, J.L.G. Fierro, Catal. Rev.-Sci. Eng. 38 (2) (1996) 161.
[9] H. Schweiger, P. Raybaud, G. Kresse, H. Toulhoat, J. Catal. 207 (2002) 76.
[10] P. Raybaud, J. Hafner, G. Kresse, S. Kasztelan, H. Toulhoat, J. Catal. 189 (2000) 129.
[11] P. Raybaud, J. Hafner, G. Kresse, S. Kasztelan, H. Toulhoat, J. Catal. 190 (2000) 128.
[12] A. Travert, C. Dujardin, F. Mauge, S. Cristol, J.-F. Paul, E. Payen, D. Bougeard, Catal. Today 70 (2001) 255.
[13] L.S. Byskov, J.K. Nørskov, B.S. Clausen, H. Topsøe, J. Catal. 187 (1999) 109.
[14] M.L. Vrinat, C.G. Gachet, L. De Mourgues, in: B. Imelick, C. Naccache, Y. Ben Taarit, J.C. Vedrine, G. Coudurier, H. Praliaud (Eds.), Catalysis by Zeolites, Elsevier, Amsterdam, 1980, p. 219.
[15] R. Cid, F. Orellana, A.L. Agudo, Appl. Catal. 32 (1987) 327.
[16] W.J.J. Welters, V.H.J. De Beer, R.A. Van Santen, Appl. Catal. A 119 (1994) 253.
[17] W.J.J. Welters, G. Vorbeck, H.W. Zandbergen, J.W. De Haan, V.H.J. De Beer, R.A. Van Santen, J. Catal. 150 (1994) 155.
[18] Y. Ono, in: B. Imelik, C. Naccache, Y. Ben Taarit, J.C. Vedrine, G. Coudurier, H. Praliaud (Eds.), Catalysis by Zeolites, Elsevier, Amsterdam, 1980, p. 19.
[19] C.L. Garcia, J.A. Lercher, J. Mol. Struct. 293 (1993) 235.
[20] S.Y. Yu, W. Li, E. Iglesia, J. Catal. 187 (1999) 257.
[21] R.M. Barrer, Zeolite and Clay Minerals as Sorbents and Molecular Sieves, Academic Press, New York, 1978.
[22] R.A. Van Santen, G.J. Kramer, Chem. Rev. 95 (1995) 637.
[23] R.A. Van Santen, X. Rozanska, in: A. Chakraborty (Ed.), Molecular Modeling and Theory in Chemical Engineering, in: Advances in Chemical Engineering, Vol. 28, Academic Press, New York, 2001, p. 399.
[24] J.M. Thomas, W.J. Thomas, in: Principles and Practice of Heterogeneous Catalysis, VCH, Weinheim, 1997.
[25] S.M. Csicsery, Zeolites 4 (1984) 202.
[26] N.Y. Chen, T.F. Degnan Jr., C.M. Smith, in: Molecular Transport and Reaction in Zeolites, Design and Applications of Shape Selective Catalysts, VCH, Weinheim, 1994, p. 195.

[27] D. Fraenkel, M. Levy, J. Catal. 118 (1989) 10.
[28] T.-C. Tsai, S.-B. Liu, I. Wang, Appl. Catal. A 181 (1999) 355.
[29] P.B. Venuto, Micropor. Matter. 2 (1994) 297.
[30] X. Saintigny, R.A. Van Santen, S. Clémendot, F. Hutschka, J. Catal. 183 (1999) 107.
[31] X. Rozanska, R.A. Van Santen, F. Hutschka, J. Catal. 200 (2001) 79.
[32] X. Rozanska, X. Saintigny, R.A. Van Santen, S. Clémendot, F. Hutschka, J. Catal. 208 (2002) 89.
[33] X. Rozanska, X. Saintigny, R.A. Van Santen, F. Hutschka, J. Catal. 202 (2001) 141.
[34] A.M. Vos, X. Rozanska, R.A. Schoonheydt, R.A. Van Santen, F. Hutschka, J. Hafner, J. Am. Chem. Soc. 123 (2001) 2799.
[35] X. Rozanska, R.A. Van Santen, F. Hutschka, J. Hafner, J. Am. Chem. Soc. 123 (2001) 7655.
[36] X. Rozanska, R.A. Van Santen, F. Hutschka, J. Hafner, J. Catal. 205 (2002) 388.
[37] X. Rozanska, R.A. Van Santen, F. Hutschka, in: M.A.C. Nascimento (Ed.), Theoretical Aspects of Heterogeneous Catalysis, Kluwer Academic, Dordrecht, 2001, p. 1.
[38] X. Rozanska, T. Demuth, Hutschka, J. Hafner, R.A. Van Santen, J. Phys. Chem. B 106 (2002) 3248.
[39] H. Klein, C. Kirschhoch, H. Fuess, J. Phys. Chem. 98 (1994) 12345.
[40] J. Sauer, M. Sierka, F. Haase, in: D.G. Truhlar, K. Morokuma (Eds.), Transition State Modeling for Catalysis, in: ACS Symp. Ser., Vol. 721, Am. Chem. Society, Washington, DC, 1999, p. 358.
[41] I. Štich, J.D. Gale, K. Terakura, M.C. Payne, J. Am. Chem. Soc. 121 (1999) 3292.
[42] G. Kresse, J. Hafner, Phys. Rev. B 48 (1993) 13115.
[43] G. Kresse, J. Hafner, Phys. Rev. B 49 (1994) 14251.
[44] G. Kresse, J. Furthmüller, Comput. Mater. Sci. 6 (1996) 15.
[45] G. Kresse, J. Furthmüller, Phys. Rev. B 54 (1996) 11169.
[46] J.P. Perdew, A. Zunger, Phys. Rev. B 23 (1981) 5048.
[47] J.P. Perdew, K. Burke, Y. Wang, Phys. Rev. B 54 (1996) 16533.
[48] G. Kresse, J. Hafner, J. Phys. Condens. Mater. 6 (1994) 8245.
[49] T. Demuth, J. Hafner, L. Benco, H. Toulhoat, J. Phys. Chem. B 104 (2000) 4593.
[50] I. Štich, J.D. Gale, K. Terakura, M.C. Payne, Chem. Phys. Lett. 283 (1998) 402.
[51] G. Mills, H. Jónsson, G.K. Schenter, Surf. Sci. 324 (1995) 305.
[52] F. Geobaldo, G.T. Palomino, S. Bordiga, A. Zecchina, C.O. Areán, Phys. Chem. Chem. Phys. 1 (1999) 561.
[53] L.A.M.M. Barbosa, R.A. Van Santen, J. Hafner, J. Am. Chem. Soc. 123 (2001) 4530.
[54] M.J. Rice, A.K. Chakraborty, A.T. Bell, J. Phys. Chem. B 104 (2000) 9987.
[55] G.N. Vayssilov, in: M.A.C. Nascimento (Ed.), Theoretical Aspects of Heterogeneous Catalysis, Kluwer Academic, Dordrecht, 2001, p. 29.
[56] X. Rozanska, R.A. Van Santen, F. Hutschka, J. Phys. Chem. B 106 (2002) 4652.
[57] X. Rozanska, R.A. van Santen, T. Demuth, F. Hutschka, J. Hafner, J. Phys. Chem. B 107 (2003) 1309.
[58] N. Brønsted, Chem. Rev. 5 (1928) 231.
[59] M.G. Evans, N.P. Polaniy, Trans. Faraday Soc. 34 (1938) 11.
[60] J.G. Ángyán, D. Parsons, Y. Jeanvoine, in: M.A.C. Nascimento (Ed.), Theoretical Aspects of Heterogeneous Catalysis, Kluwer Academic, Dordrecht, 2001, p. 77.
[61] E.J.M. Hensen, M.J. Vissenberg, V.H.J. De Beer, J.A.R. Van Veen, R.A. Van Santen, J. Catal. 163 (1996) 429.
[62] E.J.M. Hensen, H.J.A. Brans, G.M.H.J. Lardinois, V.H.J. De Beer, J.A.R. Van Veen, R.A. Van Santen, J. Catal. 192 (2000) 98.
[63] M. Neurock, R.A. Van Santen, J. Am. Chem. Soc. 116 (1994) 4427.
[64] P. Raybaud, J. Hafner, G. Kresse, H. Toulhoat, Phys. Rev. Lett. 80 (1998) 1481.
[65] E.J.M. Hensen, V.H.J. De Beer, R.A. Van Santen, in: T. Weber, R. Prins, R.A. van Santen (Eds.), Transition Metal Sulphides, Chemistry and Catalysis, in: NATO ASI Series 3, Vol. 60, Kluwer Academic, Dordrecht, 1998, p. 169.
[66] A. Corma, C. Martínez, G. Ketley, G. Blair, Appl. Catal. A 208 (2001) 135.
[67] F. Bataille, J.L. Lemberton, G. Pérot, P. Leyrit, T. Cseri, N. Marchal, S. Kasztelan, Appl. Catal. A 220 (2001) 191.